# Investigation of a stripline transmission line structure for gyromagnetic nonlinear transmission line high power microwave sources

D. V. Reale, J. M. Parson, A. A. Neuber, J. C. Dickens, and J. J. Mankowski

Citation: Rev. Sci. Instrum. **87**, 034706 (2016); doi: 10.1063/1.4942246
View online: http://dx.doi.org/10.1063/1.4942246
View Table of Contents: http://aip.scitation.org/toc/rsi/87/3
Published by the American Institute of Physics

RIGHTSLINK

# Investigation of a stripline transmission line structure for gyromagnetic nonlinear transmission line high power microwave sources

D. V. Reale,[a] J. M. Parson, A. A. Neuber, J. C. Dickens, and J. J. Mankowski
*Center for Pulsed Power & Power Electronics, Texas Tech University, Lubbock, Texas 79409, USA*

(Received 30 September 2015; accepted 6 February 2016; published online 15 March 2016)

A stripline gyromagnetic nonlinear transmission line (NLTL) was constructed out of yttrium iron garnet ferrite and tested at charge voltages of 35 kV–55 kV with bias fields ranging from 10 kA/m to 20 kA/m. Typically, high power gyromagnetic NLTLs are constructed in a coaxial geometry. While this approach has many advantages, including a uniform transverse electromagnetic (TEM) mode, simple interconnection between components, and the ability to use oil or pressurized gas as an insulator, the coaxial implementation suffers from complexity of construction, especially when using a solid insulator. By moving to a simpler transmission line geometry, NLTLs can be constructed more easily and arrayed on a single substrate. This work represents a first step in exploring the suitability of various transmission line structures, such as microstrips and coplanar waveguides. The resulting high power microwave (HPM) source operates in ultra high frequency (UHF) band with an average bandwidth of 40.1% and peak rf power from 2 MW to 12.7 MW. © *2016 AIP Publishing LLC.* [http://dx.doi.org/10.1063/1.4942246]

## I. INTRODUCTION

A gyromagnetic nonlinear transmission line (NLTL) creates microwave oscillations by inducing coherent gyromagnetic precession of the magnetic moments in a ferrimagnetic material. Details on the operation of gyromagnetic NLTLs and the underlying theory of magnetization dynamics can be found in previous work[1–8] with only a brief discussion of relevant concepts presented here.

In a gyromagnetic NLTL in microwave generation mode,[6] an axial bias is applied to align the magnetic moments of the ferrimagnetic material, followed by an incident voltage pulse to stimulate precession. The magnetic moments will process around the effective magnetic field created by the externally applied fields and the internal demagnetizing field, where only oscillations in the circumferential component of the magnetic moment $\frac{d\mathbf{M}_\phi}{dt}$ excite a TEM wave that propagates down the line. The frequency of the oscillations is determined by the magnitude of the local magnetic field $\mathbf{H}_{eff}$ seen by the individual magnetic moments.[8] A survey of existing gyromagnetic NLTLs, from the Institute of High Current Electronics (IHCE) in Tomsk Russia, MBDA UK Ltd., in Bristol UK, and Texas Tech University (TTU), is presented in Table I. The type of construction, peak power, and operating frequency is listed. All surveyed high power systems use the coaxial implementation.

As an alternative to the prevalent coaxial implementation, and in order to investigate the effect of structure on NLTL performance, a high voltage stripline based NLTL was designed and tested.

## II. NLTL STRUCTURES

Previously, high voltage gyromagnetic NLTLs were constructed in a coaxial manner.[1–6,10,11,13–16] This method of construction has many benefits including the availability of commercial toroidal ferrites, a fully circular cross section which reduces field enhancements, a natural containment structure for insulating media such as pressurized gas or dielectric oils, and a well defined TEM mode. The benefits of a coaxial structure are obvious, however, construction of devices capable of high voltage hold-off while preserving a consistent impedance to the generated microwaves is a considerable challenge; a challenge that is compounded when multiple lines are integrated into a single system. Examples of solid insulated and gas insulated coaxial NLTL designs are shown in Figure 1. Solid insulated coaxial NLTLs are constructed by plotting the ferrites inside the coaxial shell using an epoxy.[17] Extruded solid insulators introduce too many air gaps which lead to triple points inside the structure and reduced dielectric breakdown strength, thus limiting the output power of the NLTL below its theoretical maximum.

A novel approach is to use a bulk ferrite substrate as the transmission line structure, which greatly simplifies device construction. The possible choices for a bulk transmission line structure include microstrips, co-planar waveguides, and striplines. The stripline geometry was chosen due to its quasi-circular TEM mode, which is similar to the coaxial TEM mode as shown in Figure 2. This choice allows for the closest possible comparison of the performance of the stripline based NLTL with existing coaxial NLTLs.

## III. DESIGN AND CONSTRUCTION

The stripline based NLTL was designed to use existing 12.7 mm thick slabs of ferrite material. In order to reduce field enhancements, the classic stripline design was modified to include a round center conductor. To account for the modification of the inner conductor geometry when calculating the transmission line characteristic impedance $Z_0$, an

[a]david.reale@ttu.edu

 © 2016 AIP Publishing LLC

RIGHTSLINK

TABLE I. Survey of gyromagnetic NLTL sources.

| Research group | Line geometry | Charge voltage (kV) | Peak power (MW) | Center frequency (GHz) |
|---|---|---|---|---|
| IHCE [9] | Coaxial | 250 | 260 | 1.20 |
| IHCE [10] | Coaxial | 130 | 110 | 1.95 |
| MBDA [11] | Coaxial | 80 | 89.3 | 0.77 |
| TTU (NiZn)[12] | Coaxial | 40 | 8.4 | 4.10 |
| TTU (YIG) [3] | Coaxial | 40 | 2.03 | 3.01 |

electrostatic simulation in COMSOL was used to solve for the capacitance of the structure. The characteristic impedance of the transmission line can be determined from Equation (1) if the capacitance per unit length $C'$ and the propagation velocity in the transmission line $v_p$ are known. The propagation velocity used is given in Equation (2) where $c$ is the free space speed of light, $\mu_{r,sat}$ is the saturated relative permeability of the ferrite, and $\epsilon_r$ is the permittivity of the ferrite,

$$Z_0 = \frac{1}{v_p C'}, \tag{1}$$

$$v_p = \frac{c}{\sqrt{\mu_{r,sat}\epsilon_r}}. \tag{2}$$

A modal analysis was conducted using COMSOL with the chosen geometry at a frequency of 750 MHz (Fig. 3). The width of the stripline structure was chosen such that the modal TEM field was negligible at the point which the ferrite substrate ends. With the width and substrate thickness held fixed, a parametric sweep of the center conductor diameter was conducted to determine the size required for a 50 Ω line.

### A. Construction

The stripline NLTL was constructed from multiple 12.7 mm thick by 50.8 mm wide by 30.5 cm long ferrite slabs. A rounded groove was machined into one side of each slab to accommodate the center conductor. The individual ferrite slabs were compressed using two aluminum plates with a 5 mil layer of polyimide tape between the plate and ferrite for added insulation. Figure 4 shows the cross-section of the structure and the constructed NLTL is shown in Figure 5. The ferrite slabs were machined from Yttrium Iron Garnet (YIG) ferrite.

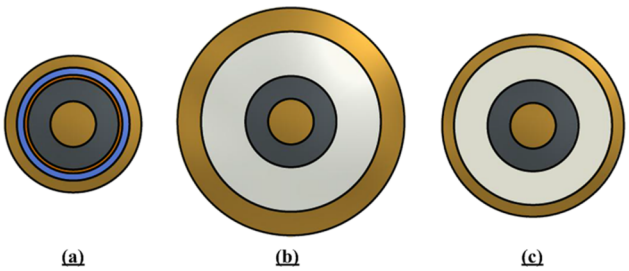


FIG. 1. Relative scale of 50 Ω NLTLs constructed using (a) $SF_6$ gas and polyimide insulation, (b) an epoxy insulation, and (c) a silicone elastomer insulation.

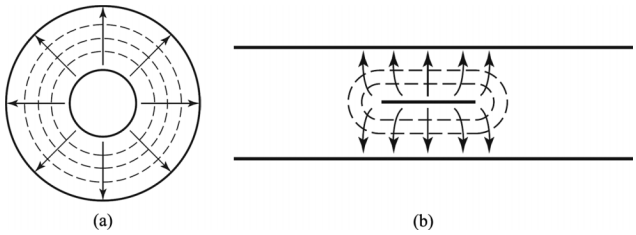


FIG. 2. (a) Coaxial TEM Mode. (b) TEM Mode in a stripline.

## IV. EXPERIMENTAL SETUP

A test setup was built to evaluate the YIG stripline NLTL. Figure 6 shows the system schematic for the test setup used. A 1.2 nF capacitor is charged to the specified voltage and then discharged via a gas purge operated pressurized spark gap into the stripline NLTL. Dry air pressurized to 60 psig (550 kPa) was used in the spark gap. The output of the NLTL is connected to a 50 Ω resistive load via a length of LMR-600 coaxial cable that serves as a delay line. A large solenoid was constructed to slide over the entire stripline assembly. The input and output connections were made using standard DIN 7/16 connectors pressurized with Sulfur Hexaflouride ($SF_6$) gas[3,6] at 70 psig (584 kPa). In order to prevent flashover across the ferrite surface, the entire test setup was placed in transformer oil. Figure 7 shows the spark gap, connected stripline NLTL, and the solenoid before the system was placed in oil.

### A. Integrated D-Dot probe

A simple D-Dot probe consisting of an SMA bulkhead connector was built into the stripline structure (Figure 5). To calibrate the integrated D-Dot, the stripline was connected to a Agilent E8364B PNA network analyzer. The input port of the NLTL was connected to Port 1, the SMA bulkhead connector was connected to Port 2, and the output of the NLTL was connected to a broadband 50 Ω load. During system operation the NLTL is saturated by the external biasing field and the incident high voltage pulse. Therefore, in order to replicate the conditions seen by the probe during a high voltage pulse, a 16 turn solenoid coil was constructed to apply a magnetic field of 200 kA/m to saturate the ferrites while the network analyzer performed the frequency sweep. A picture of the calibration setup is shown in Figure 8 and the measured $S_{21}$ is given in Figure 9.

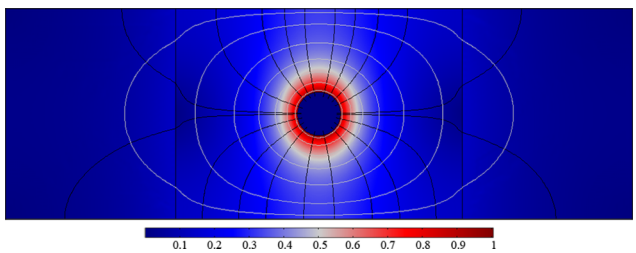


FIG. 3. Normalized modal electric field inside the ferrite substrate at 750 MHz. Black lines represent the electric field contours and white lines the magnetic field contours.

RIGHTSLINK

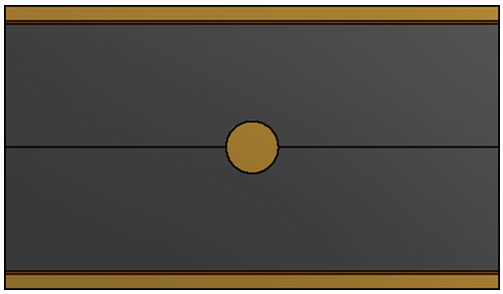

FIG. 4. Cross-section of the stripline NLTL with a simulated impedance of 50.28 Ω.

The attenuation of a D-Dot is a function of frequency with the probe being more sensitive at higher frequencies. The measured response of the probe has peaks and valleys that when applied to the measured rf signal may overestimate or underestimate the contribution of a given frequency. A linear fit, shown in Figure 9, was applied using a constant scale factor that represents the equivalent area of the D-Dot ($A_{eq} \approx 0.59$ cm$^2$) with the linear fit chosen conservatively to err on the side of underestimating the reported rf power. The raw voltage signals are filtered with a 4th order Butterworth band-pass filter between 500 MHz and 2 GHz. A FFT is performed on the filtered signal and the FFT is scaled by the linear fit of the D-Dot response; an IFFT is then performed to recover the time domain signal.

## V. RESULTS

The initial charge voltage and the axially applied bias field were swept to determine the optimum operation point. Table II shows the parameters tested with a single shot recorded for each parameter.

Peak rf power, center frequency, and bandwidth are observed for each shot. The instantaneous peak rf power is calculated using peak voltage of the filtered signal divided by the characteristic impedance of the stripline, taken to be nominally 50 Ω, according to Equation (3),

$$P_{rf,peak} = \frac{V_{peak}^2}{Z_0}. \tag{3}$$

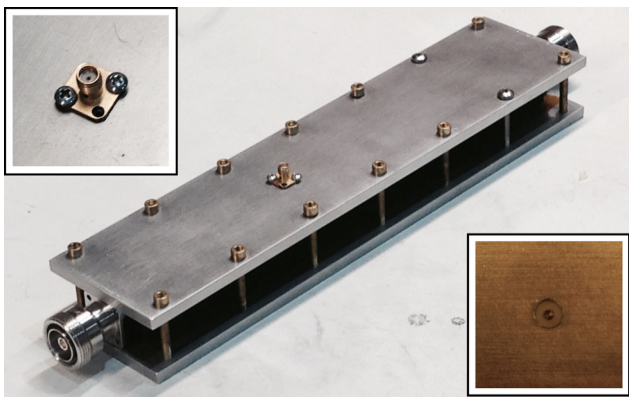

FIG. 5. Constructed stripline NLTL with input and output DIN 7/16 connectors and integrated SMA D-Dot probe (inset).

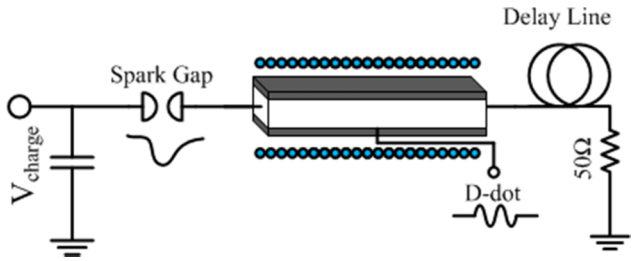


FIG. 6. Schematic of the test setup. A gas purge operated spark gap dumps a 1 nF capacitor into the stripline NLTL structure. A D-Dot probe is integrated into the structure.

Figure 10 plots the peak rf power as a function of applied bias field for each charge voltage. The power increases with increasing charge voltage while the power is maximum for bias fields of 12.4 kA/m. This trend is similar to coaxial constructed lines.[6] Also shown in Figure 10 are the best performing YIG coaxial lines previously tested,[3] including the closest comparison available, a 40 kV charge voltage at a 15 kA/m bias in a 76.2 cm long coaxial NLTL. The best coaxial peak rf power achieved was 2 MW at a bias of 15 kA/m with a frequency of 3 GHz. The peak rf power observed in the stripline NLTL at 40 kV is 7.4 MW at a bias of 10 kA/m with a frequency of 771 MHz. Increasing the bias field aligns the domains of the ferrimagnetic material allowing for coherent precession of the magnetic moments, however, by further increasing the bias field the moments process around an effective magnetic field $H_{eff}$ that is more closely aligned to the axial direction; as a result there is a smaller component of magnetic in the azimuthal direction to excite the TEM mode of the stripline. Waveforms of the best performing shots identified in Figure 10 are shown in Figure 11.

The center frequency is plotted as a function of bias field for each charge voltage in Figure 12. As the bias field and charge voltage increase, the center frequency increases. This trend is expected since the frequency of precession of a gyromagnetic NLTL is a function of the magnetic field as discussed in Section I.[6,8,13] The bandwidth of the rf signal is also given in Figure 12. An interesting trend is that the signal becomes more narrowband at all charge voltages with increasing applied bias. This could indicate stronger alignment of the magnetic domains with the applied field causing more coherent precession of the magnetic moments. The fact that this does not increase the peak rf power observed may be explained by the effective field being held down in the axial direction as described in the preceding paragraph. A higher incident voltage pulse at these bias field levels may therefore yield higher output power and a more narrowband rf pulse.

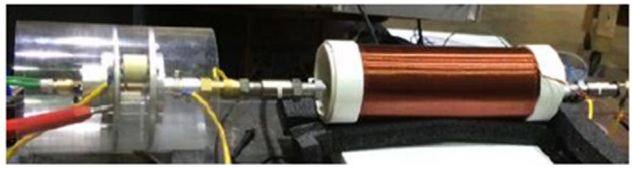

FIG. 7. Picture of spark gap, solenoid, and stripline NLTL (within solenoid) before the test setup is immersed in transformer oil.

RIGHTSLINK

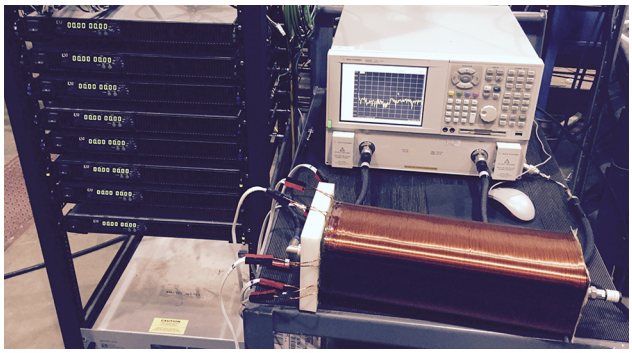

FIG. 8. D-Dot calibration setup. The network analyzer excites the input port while a large solenoid coil driven by 8 1500 W current supplies saturates the ferrite slabs.

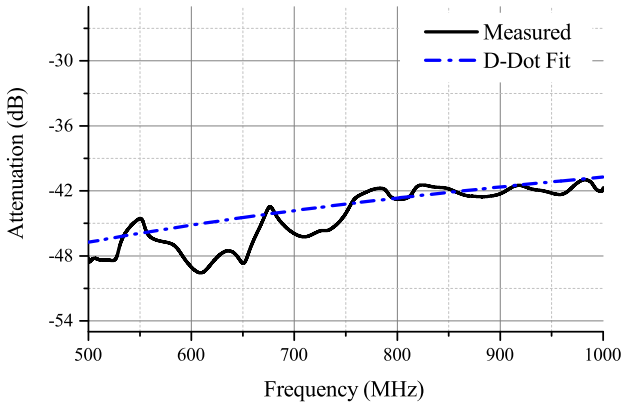


FIG. 9. Measured $S_{21}$ of the D-Dot probe in black and a linear fit shown as a blue dashed line.

TABLE II. Test matrix.

| Charge voltage (kV) | Bias field (kA/m) | Material |
|---|---|---|
| 35 | 5.2, 7.6, 10.0, 15.6, 17.2 | YIG |
| 40, 50, 55 | 5.2, 7.6, 10.0, 12.4, 15.6, 17.2 | YIG |

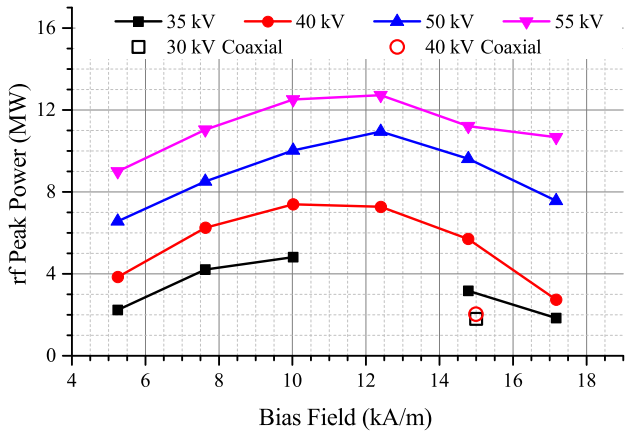


FIG. 10. Peak power for each charge voltage vs applied bias field. Best performing coaxial NLTLs with YIG ferrite are plotted as red hollow circles for 40 kV and a black hollow square for 30 kV for comparison.[3]

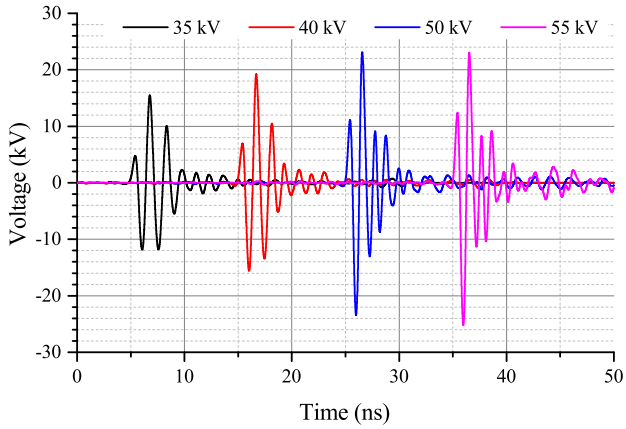


FIG. 11. Best performing rf waveforms for each charge voltage artificially time shifted for clarity.

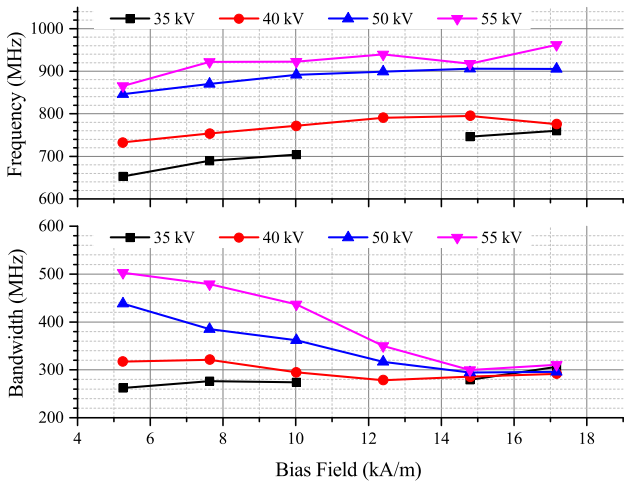


FIG. 12. Center frequency and bandwidth for each charge voltage as a function of applied bias field.

## VI. CONCLUSION

A novel stripline based NLTL topology was constructed out of YIG ferrite and tested. Output rf power levels from 2 MW to 1.27 MW were achieved with charge voltages from 35 kV to 55 kV at center frequencies from 620 MHz to 960 MHz. The resulting trends in both frequency and power as a function of incident voltage and bias fields are consistent with trends observed in coaxial NLTLs. The stripline NLTL generated higher rf power in a shorter line than a coaxial version with the same applied bias and incident voltage magnitude. Future work will be focused on relating the generated magnitude of the generated rf power with the volume of ferrite material in the structure and the alignment of the effective magnetic field within the ferrite.

## ACKNOWLEDGMENTS

This work was funded by the Office of Naval Research (ONR) No. SBIR N141-060 and conducted in conjunction with MetaMagnetics, Inc. of Canton, MA.

RIGHTSLINK

[1]N. Seddon, C. R. Spikings, and J. E. Dolan, "Rf pulse formation in nonlinear transmission lines," in 16th IEEE International Pulsed Power Conference, 2007.
[2]J. E. Dolan and H. R. Bolton, "Shock front development in ferrite-loaded coaxial lines with axial bias," IEE Proc.: Sci., Meas. Technol. **147**, 237 (2000).
[3]D. V. Reale, J.-W. B. Bragg, N. R. Gonsalves, J. M. Johnson, A. A. Neuber, J. C. Dickens, and J. J. Mankowski, "Bias-field controlled phasing and power combination of gyromagnetic nonlinear transmission lines," Rev. Sci. Instrum. **85**, 054706 (2014).
[4]J.-W. B. Bragg, J. C. Dickens, and A. A. Neuber, "Material selection considerations for coaxial, ferrimagnetic-based nonlinear transmission lines," J. Appl. Phys. **113**, 064904 (2013).
[5]I. V. Romanchenko, V. V. Rostov, A. I. Klimov, I. K. Kurkan, A. V. Gunin, V. I. Koshelev, K. N. Sukhushin, Y. A. Andreev, and V. Y. Konev, "Effective irradiation of high-power RF pulses from gyromagnetic nonlinear transmission lines," in 19th IEEE Pulsed Power Conference (PPC), 2013.
[6]D. V. Reale, "Coaxial ferrimagnetic based gyromagnetic nonlinear transmission lines as compact high power microwave sources," Ph.D. thesis, Texas Tech University, 2013.
[7]W. B. Hatfield and B. A. Auld, "Electromagnetic shock waves in gyromagnetic media," J. Appl. Phys. **34**, 2941 (1963).
[8]J. Stohr and H. C. Siegmann, *Magnetism* (Springer, Berlin Heidelberg, 2006).
[9]I. V. Romanchenko, V. V. Rostov, V. P. Gubanov, A. S. Stepchenko, A. V. Gunin, and I. K. Kurkan, "Repetitive sub-gigawatt rf source based on gyromagnetic nonlinear transmission line," Rev. Sci. Instrum. **83**, 074705 (2012).
[10]M. R. Ulmaskulov, M. S. Pedos, S. N. Rukin, K. A. Sharypov, V. G. Shpak, S. A. Shunailov, M. I. Yalandin, I. V. Romanchenko, and V. V. Rostov, "High repetition rate multi-channel source of high-power rf-modulated pulses," Rev. Sci. Instrum. **86**, 074702 (2015).
[11]S. Chadwick, N. Seddon, and S. Rukin, "A novel solid-state hpm source based on a gyromagnetic nltl and sos-based pulse generator," in 2011 IEEE Pulsed Power Conference, 2011.
[12]J.-W. B. Bragg, J. C. Dickens, and A. A. Neuber, "Ferrimagnetic nonlinear transmission lines as high-power microwave sources," IEEE Trans. Plasma Sci. **41**, 232–237 (2013).
[13]J.-W. B. Bragg, W. W. Sullivan, D. Mauch, A. A. Neuber, and J. C. Dickens, "All solid-state high power microwave source with high repetition frequency," Rev. Sci. Instrum. **84**, 054703 (2013).
[14]I. V. Romanchenko, V. V. Rostov, A. V. Gunin, and V. Y. Konev, "High power microwave beam steering based on gyromagnetic nonlinear transmission lines," J. Appl. Phys. **117**, 214907 (2015).
[15]Y. Abe and Y. Minamitani, "Development of a RF burst pulse generator using a non-linear transmission line for cancer treatment," in 2012 IEEE International Power Modulator and High Voltage Conference (IPMHVC), 2012.
[16]J. M. Johnson, D. V. Reale, W. H. Cravey, R. S. Garcia, D. H. Barnett, A. A. Neuber, J. C. Dickens, and J. J. Mankowski, "Material selection of a ferrimagnetic loaded coaxial delay line for phasing gyromagnetic nonlinear transmission lines," Rev. Sci. Instrum. **86**, 084702 (2015).
[17]R. C. Solarski, D. V. Reale, J.-W. B. Bragg, A. A. Neuber, S. L. Holt, J. J. Mankowski, and J. C. Dickens, "High voltage solid dielectric coaxial ferrimagnetic nonlinear transmission line," in *2013 19th IEEE Pulsed Power Conference (PPC)* (Institute of Electrical and Electronics Engineers, 2013), pp. 1–3.

RIGHTSLINK